Modelling of flexible bodies with minimal coordinates by means of the co-rotational formulation

Olivier Verlinden[1], Hoai Nam Huynh[2] and Edouard Rivière[3]

[1]*Department of Theoretical mechanics, Dynamics and Vibration, University of Mons, Olivier.Verlinden@umons.ac.be*
[2]*Department of Theoretical mechanics, Dynamics and Vibration, University of Mons, HoaiNam.Huynh@umons.ac.be*
[3]*Department of Machine Design, Production and Manufacturing, University of Mons, Edouard.Riviere@umons.ac.be*

ABSTRACT

This paper is concerned with the extension of the minimal coordinates approach to flexible bodies. When using minimal coordinates, the number of configuration parameters corresponds exactly to the number of degrees of freedom and they can be chosen arbitrarily as far as there is a one-to-one relationship between the configuration of the system and the configuration parameters. The equations of motion are obtained from the description of the translational and rotational motion of a frame attached to each body in terms of the chosen configuration parameters, and from the forces acting on each body. The extension to the simulation of flexible bodies naturally leads to a description of the motion of a flexible body from the one of its nodes. However, the relationship between the latter and the full internal motion of the body is not unique and is the subject of a lot of developments. It was then decided to systematically treat flexible bodies as superelements, implemented according to the corotational approach, with a floating corotational frame. This allows to model any flexible body from its mass and stiffness matrices obtained from any available finite element code. Moreover, it doesn't impose any restriction on the kinematics of the nodes which can then be expressed indifferently from absolute or relative coordinates as usually encountered with minimal coordinates. After a description of the adopted framework, the paper develops the equations of motion. Some test examples will then be presented, where the proposed approach will be compared to the ones obtained with the classical body reference frame approach and results from the literature. In some cases, the influence of the chosen corotational frame will be analysed.

1 Introduction

Kinematics is an important step of multibody modelling. It consists in expressing the motion of the bodies in terms of the configuration parameters and their first and second time derivatives. The configuration parameters themselves can be chosen according to different types of coordinates[1]: relative, absolute, natural, minimal or nodal coordinates, the choice influencing the principle used to build the equations of motion, the form of the latter (ODE or DAE, sparse, ...) and consequently the numerical methods expected to deal with these equations. Prof. Hiller[2] was the main contributor to the approach based on minimal coordinates. In this case, the configuration parameters are chosen freely as far as they are independent and that their number is equal to the number of degrees of freedom of the system. This approach is also currently used at the university of Mons, through the framework `EasyDyn`[3], which was initially developed for teaching purposes but also contributed successfully to several research projects[4].

In a project launched recently about robotic machining, the need appeared to introduce flexible bodies. The flexibility of the robot is indeed a key aspect when assessing the stability of the machining process. Although we could have switched to one of the free tools available on the web (`MBDyn`, `Hotint`, ...), it also appeared necessary to keep the scalability and our perfect mastery of `EasyDyn` as several other particular features must be introduced: computation of cutting forces[5], updating of the geometry of the machined part, joint compliance, actuators and

controllers modelling. The problem of geometry updating is particularly tricky as it is not reversible and must be processed explicitly while the equations of motion are integrated by an implicit solver.

The first section of this paper will be devoted to the analysis of the different options to model flexible bodies and their advantages and shortcomings with respect to the minimal coordinates philosophy. In the next section, the equations of motion will be constructed for the adopted solution, i.e. the modelling of flexible bodies as superelements introduced through the corotational approach, with a description of the motion of the flexible body through the one of its nodes and of the corotational frame, in terms of the chosen configuration parameters. Several examples will then be presented, where the proposed approach will be compared to the ones obtained with the classical body reference frame approach and results from the literature. In some cases, the influence of the chosen corotational frame will be analysed.

2 Flexible bodies with minimal coordinates through the corotational approach

2.1 Minimal coordinates and rigid bodies

The approach based on minimal coordinates[2] assumes that the user develops explicitly the kinematics of all bodies in function of the chosen configuration parameters. The latter can be chosen freely as far as they are related to the configuration of the system by a "one to one" relationship, which namely implies that they are independent. The solution is not necessarily unique: as shown in figure 1, the motion of a double pendulum can be described by the 2 parameters θ_1 and θ_2, but θ_2, which is a relative angle, can be replaced by α_2, which is an absolute angle. In the same way, the motion of the slider crank mechanism of figure 1 can be expressed in terms of the only angle α.
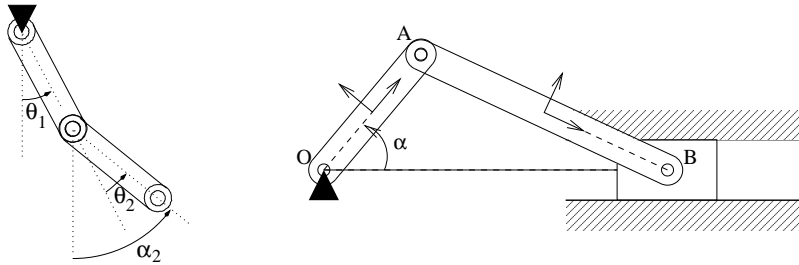

Fig. 1: Examples of sets of minimal coordinates

There are different ways to implement the approach based on minimal coordinates. In `EasyDyn` [3], which is a C++ library, the user must write a C++ application where the kinematics is programmed in the specific routine `ComputeMotion`. The latter consists of the expressions of the position, orientation and translational and rotational velocities and accelerations of each body i, in terms of the configuration parameters $\mathbf{q}$ and their first and second time derivatives $\dot{\mathbf{q}}$ and $\ddot{\mathbf{q}}$. In parallel, the user describes in another specific routine `AddAppliedEfforts` all forces exerted on each body. From this information, the n_{cp} equations of motion of a system owning n_B bodies and n_{cp} configuration parameters can be built in the following form, which derives from the application of the d'Alembert's principle

$$\sum_{i=1}^{n_B} \left[\mathbf{d}^{i,j} \cdot (\mathbf{R}_i - m_i \mathbf{a}_i) + \boldsymbol{\theta}^{i,j} \cdot (\mathbf{M}_{Gi} - \boldsymbol{\Phi}_{G_i} \dot{\boldsymbol{\omega}}_i - \boldsymbol{\omega}_i \times \boldsymbol{\Phi}_{G_i} \boldsymbol{\omega}_i) \right] = 0 \quad j = 1, n_{cp} \tag{1}$$

with m_i and $\boldsymbol{\Phi}_{G_i}$ the mass and the central inertia tensor of body i; $\mathbf{R}_i$ and $\mathbf{M}_{Gi}$ the resultant force and moment, at the center of mass G_i, of all applied efforts exerted on body i; $\mathbf{v}_i$ and $\mathbf{a}_i$ the velocity and acceleration of the center of gravity of body i; $\boldsymbol{\omega}_i$ the rotational velocity of body i; and $\mathbf{d}^{i,j}$ and $\boldsymbol{\theta}^{i,j}$ the partial contributions of $\dot{q}_j$ in the translational and rotational velocities of body i respectively

$$\mathbf{v}_i = \sum_{j=1}^{n_{cp}} \mathbf{d}^{i,j} \cdot \dot{q}_j \qquad \boldsymbol{\omega}_i = \sum_{j=1}^{n_{cp}} \boldsymbol{\theta}^{i,j} \cdot \dot{q}_j \tag{2}$$
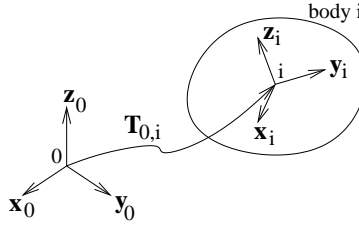
Fig. 2: Reference frame of a body and its situation with respect to the global reference frame

Practically, the position and orientation of body i are expressed through the homogeneous transformation matrix $\mathbf{T}_{0,i}$ giving the situation of the frame attached to the body with respect to the global reference frame 0 (fig 2). A significant advantage of homogeneous transformation matrices is the possibility to express the motion along a kinematic chain as the product of matrices representing the succession of elementary displacements and/or rotations, as for example

$$\mathbf{T}_{0,i} = \mathbf{T}_{rotz}(\boldsymbol{q}_1) \cdot \mathbf{T}_{disp}(0, L_1, 0) \cdot \mathbf{T}_{rotx}(\boldsymbol{q}_2) \cdot \mathbf{T}_{disp}(L_2, 0, 0) \tag{3}$$

Moreover, to help the users, a symbolic tool called `CAGeM` (Computer Aided Generation of Motion) generates the expressions of velocities and accelerations by symbolic differentiation. `CAGeM` was initially implemented under `MuPAD` and a port under `Python/sympy` is under development.

2.2 Flexible bodies and minimal coordinates

If the motion of a rigid body is naturally described through the one of a coordinate system attached to it, it naturally appears that the motion of a flexible body should be defined by **the one of its nodes**. To make it clear, the motion of a flexible beam (figure 3) would be defined by the one of the two coordinate systems attached to its end nodes. At that point, it is of interest to note that a major difference between minimal coordinates and relative or Cartesian coordinates is that the formulation is not related at all to the topology of the mechanical system. Relative coordinates generally exploit kinematic chains, the configuration parameters corresponding to joint variables. Cartesian coordinates systematically involve absolute configuration parameters and introduce all joints through constraints. Besides, minimal coordinates can mix relative and absolute coordinates (cf. double pendulum) and it would be very difficult to define whether α is a relative or absolute coordinate for the rod or the piston of the slider crank mechanism. So the chosen approach should permit to express the motion of the end nodes of a beam either from their absolute motion or from the absolute motion of one of the nodes and the relative motion of the second with respect to the first one.
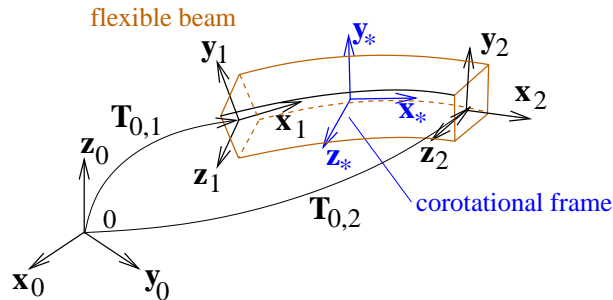

Fig. 3: Kinematics of a flexible beam

Two main approaches are generally found to express the motion of a flexible body

- the local body reference frame approach where the motion of the body is the superimposition of a rigid body (undeformed) motion and a deformation, generally assumed small, with respect to the latter (figure 4);

3

- the full finite element approach where the motion of the flexible body is expressed directly from the translational and rotational motion of its nodes, which assumes a consistent parametrization of the rotations and shape functions valid for large displacements.
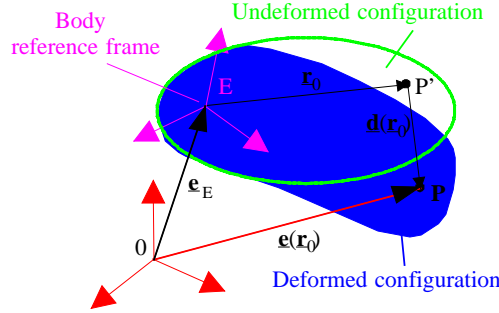

Fig. 4: Kinematics of a flexible body with the local body reference frame

Taking into account the first paragraph, the approach based on the local body reference frame would not be natural as it imposes to use relative coordinates for the description of the deformed configuration and would need to provide information on the component modes used to express the deformation. On the other hand, the full finite element approach writes equations of motion for specific translation and rotation parameters. The advantage is that, in this case, the internal motion is precisely defined by the element shape functions. The parametrization is also imposed but the equations of motion could be reformulated through a kinematic transformation between finite element parameters and the minimal coordinates. However, it would make the approach inefficient, due to the ignorance of the topology, and would oblige to implement all types of elements (beams, plates, tetrahaedrons, bricks, ...).

Taking into account these remarks, the retained approach to introduce flexible bodies in `EasyDyn` relies on

- the formulation of the dynamics of the flexible bodies through the so-called co-rotational formulation ([6, 7]), the co-rotating frame being floating[7] and not necessarily attached to one of the nodes;

- a free description of the motion of the nodes and the co-rotating frame, through a homogeneous transformation matrix, assumingly expressed in terms of the chosen configuration parameters.

2.3 Expression of the kinetic energy with the corotational formulation

The magic idea of the co-rotational approach is to express the kinetic energy of a "N nodes" flexible body (a superelement), as

$$
T = \frac{1}{2}
\begin{Bmatrix}
\{\mathbf{v}_1\}_* \\
\{\boldsymbol{\omega}_1\}_* \\
\vdots \\
\{\mathbf{v}_N\}_* \\
\{\boldsymbol{\omega}_N\}_*
\end{Bmatrix}^T
\cdot
\begin{bmatrix}
\mathbf{M}_{T1,T1} & \mathbf{M}_{T1,R1} & : & \mathbf{M}_{T1,TN} & \mathbf{M}_{T1,RN} \\
\mathbf{M}_{R1,T1} & \mathbf{M}_{R1,R1} & : & \mathbf{M}_{R1,TN} & \mathbf{M}_{R1,RN} \\
\vdots & \vdots & : & \vdots & \vdots \\
\mathbf{M}_{TN,T1} & \mathbf{M}_{TN,R1} & : & \mathbf{M}_{TN,TN} & \mathbf{M}_{TN,RN} \\
\mathbf{M}_{RN,T1} & \mathbf{M}_{RN,R1} & : & \mathbf{M}_{RN,TN} & \mathbf{M}_{RN,RN}
\end{bmatrix}
\cdot
\begin{Bmatrix}
\{\mathbf{v}_1\}_* \\
\{\boldsymbol{\omega}_1\}_* \\
\vdots \\
\{\mathbf{v}_N\}_* \\
\{\boldsymbol{\omega}_N\}_*
\end{Bmatrix}
\tag{4}
$$

i.e. from the native mass matrix of the finite element model of the flexible body and the translational and rotational velocities of the N "nodes" projected in a reference corotational frame * following (rotating with) the flexible body[1]. Initially[6], the corotational frame was attached to one of the nodes. More recently[7], Cardona proposed to use instead a floating corotational frame obtained by averaging the translational and rotational parameters of the body nodes.

---

[1]While $\mathbf{v}$ denotes a vector characterized by a magnitude, a direction and a sense, $\{\mathbf{v}\}_*$ denotes the 3x1 matrix gathering the coordinates of vector $\mathbf{v}$ in coordinate system *

The main advantage of the approach is that any kind of flexible body can be modelled, as soon as its finite element model is available, from which the mass and stiffness properties can be retrieved. The only condition on the finite element model is that each node involves the 3 displacements and the 3 rotations of each node. The approach is not fully consistent as equation 4 corresponds to an interpolation of the velocity field through the shape functions of the superelement, also used at displacement level. As soon as the shape functions are able to span the rigid body modes, the expression is exact when the body is undeformed. However, the discrepancy increases with the magnitude of the deformation and the rotational velocity of the body. As a conclusion, the corotational approach is suitable when deformations and rotation speeds are small, which is the case of our application. The results are also better if the corotational frame is located near the center of mass of the deformed body[7].

Let us note that the rigid body can be considered as a "one node" element, for which the submatrices would take the following form if the node is located at the center of mass

$$\mathbf{M}_{T1,T1} = m\mathbf{I} \qquad \mathbf{M}_{T1,R1} = \mathbf{M}_{R1,T1} = 0 \qquad \mathbf{M}_{R1,R1} = \mathbf{\Phi}_G \tag{5}$$

3 Contribution of a flexible body to the equations of motion

The purpose of this section is to develop the equations of motion of a multibody system comprising flexible bodies, in a shape as close as possible to equation 1 related to rigid bodies.

3.1 Contribution of the inertia forces in the equations of motion

The contribution of the inertia forces in the equations of motion will be obtained from the Lagrange's theorem, stipulating that the generalized inertia force relative to configuration parameter q_l can be obtained from the kinetic energy by

$$Q_l(-m\vec{a}) = -\frac{d}{dt}\left(\frac{\partial T}{\partial \dot{q}_l}\right) - \frac{\partial T}{\partial q_l} \tag{6}$$

Let us first reformulate the expression of the kinetic energy given in equation 4 as

$$T = \frac{1}{2}\sum_{i=1}^{N}\sum_{j=1}^{N}\left(\mathbf{v}_i \cdot \mathbf{M}_{T_i,T_j}\mathbf{v}_j + \mathbf{v}_i \cdot \mathbf{M}_{T_i,R_j}\boldsymbol{\omega}_j + \boldsymbol{\omega}_i \cdot \mathbf{M}_{T_i,R_j}\boldsymbol{\omega}_j + \boldsymbol{\omega}_i \cdot \mathbf{M}_{R_i,R_j}\boldsymbol{\omega}_j\right) \tag{7}$$

in which $\mathbf{M}_{T_i,T_j}$, $\mathbf{M}_{T_i,R_j}$, $\mathbf{M}_{R_i,T_j}$ and $\mathbf{M}_{R_i,R_j}$ can be considered as tensors, which are constant in the corotational frame.

Like for the rigid bodies, the velocities $\mathbf{v}_i$ and $\boldsymbol{\omega}_i$ of each node i of the flexible body, as well as the velocities $\mathbf{v}_*$ and $\boldsymbol{\omega}_*$ of the corotational frame, can be expressed from the partial velocities $\mathbf{d}_{i,l}$, $\boldsymbol{\theta}_{i,l}$, $\mathbf{d}_{*,l}$ and $\boldsymbol{\theta}_{*,l}$, and the time derivatives of the n_{cp} configuration parameters

$$\mathbf{v}_i = \sum_{i=1}^{n_{cp}}\mathbf{d}_{i,l}\dot{q}_l \qquad \boldsymbol{\omega}_i = \sum_{i=1}^{n_{cp}}\boldsymbol{\theta}_{i,l}\dot{q}_l \qquad \mathbf{v}_* = \sum_{i=1}^{n_{cp}}\mathbf{d}_{*,l}\dot{q}_l \qquad \boldsymbol{\omega}_* = \sum_{i=1}^{n_{cp}}\boldsymbol{\theta}_{*,l}\dot{q}_l \tag{8}$$

As for the rigid bodies, the velocities, partial velocities and accelerations can be obtained by symbolic differentiation of the homogeneous transformation matrices $\mathbf{T}_{0,i}$ giving the situation of each node i with respect to the global reference frame.

The application of the Lagrange's theorem leads to the following contribution of the inertia forces:

$$Q_l(-m\mathbf{a}) = \sum_{i=1}^{N}\left(\mathbf{R}_i(-m\mathbf{a})\cdot\mathbf{d}_{i,l} + \mathbf{M}_i(-m\mathbf{a})\cdot\boldsymbol{\theta}_{i,l}\right) + \mathbf{M}_*(-m\mathbf{a})\cdot\boldsymbol{\theta}_{*,l} \tag{9}$$

5

where $\mathbf{R}_i(-m\mathbf{a})$ and $\mathbf{M}_i(-m\mathbf{a})$ represent the equivalent force respectively torque exerted on node i (or corotational frame *) by the inertia reactions, computed as

$$\mathbf{R}_i(-m\mathbf{a}) = -\sum_{j=1}^{N} \left[\mathbf{M}_{T_i,T_j}(\mathbf{a}_j - \boldsymbol{\omega}_* \times \mathbf{v}_j) + \mathbf{M}_{T_i,R_j}(\dot{\boldsymbol{\omega}}_j - \boldsymbol{\omega}_* \times \boldsymbol{\omega}_j) + \boldsymbol{\omega}_* \times (\mathbf{M}_{T_i,T_j}\mathbf{v}_j + \mathbf{M}_{T_i,R_j}\boldsymbol{\omega}_j) \right] \tag{10}$$

$$\mathbf{M}_i(-m\mathbf{a}) = -\sum_{j=1}^{N} \left[\mathbf{M}_{R_i,T_j}(\mathbf{a}_j - \boldsymbol{\omega}_* \times \mathbf{v}_j) + \mathbf{M}_{R_i,R_j}(\dot{\boldsymbol{\omega}}_j - \boldsymbol{\omega}_* \times \boldsymbol{\omega}_j) + (\boldsymbol{\omega}_* - \boldsymbol{\omega}_i) \times (\mathbf{M}_{R_i,T_j}\mathbf{v}_j + \mathbf{M}_{R_i,R_j}\boldsymbol{\omega}_j) \right] \tag{11}$$

In the same way, the inertia forces bring a contribution equivalent to a torque $\mathbf{M}_*(-m\mathbf{a})$ exerted on the corotational frame $*$ given by

$$\mathbf{M}_*(-m\mathbf{a}) = -\sum_{i=1}^{N}\sum_{j=1}^{N} \left[\mathbf{v}_i \times (\mathbf{M}_{T_i,T_j}\mathbf{v}_j) + \boldsymbol{\omega}_i \times (\mathbf{M}_{R_i,R_j}\boldsymbol{\omega}_j) + \boldsymbol{\omega}_i \times (\mathbf{M}_{R_i,T_j}\mathbf{v}_j) + \mathbf{v}_i \times (\mathbf{M}_{T_i,R_j}\boldsymbol{\omega}_j) \right] \tag{12}$$

The previous terms are calculated from their projection in the corotational frame, as the mass matrices are expected to rotate with this frame.

3.2 Contribution of gravity

Contribution of gravity is naturally included in the equations of motion through the inertia terms by replacing in equations 10 to 11 the acceleration $\mathbf{a}_j$ by $\mathbf{a}_j - \mathbf{g}$. The equivalent force and moment on node i then correspond to

$$\mathbf{R}_i(\mathbf{g}) = \left(\sum_{j=1}^{N} \mathbf{M}_{T_i,T_j} \right) \mathbf{g} \tag{13}$$

$$\mathbf{M}_i(\mathbf{g}) = \left(\sum_{j=1}^{N} \mathbf{M}_{R_i,T_j} \right) \mathbf{g} \tag{14}$$

and the resulting generalized force associated with $\boldsymbol{q}_l$ reads

$$Q_l^{gravity} = \sum_{i=1}^{N} \left(\mathbf{R}_i(\mathbf{g}) \cdot \mathbf{d}_{i,l} + \mathbf{M}_i(\mathbf{g}) \cdot \boldsymbol{\theta}_{i,l} \right) \tag{15}$$

3.3 Contribution of elastic forces

Assuming small deformations, the elastic forces are computed from the finite element stiffness matrix of the superelement, considered in the axes of the corotational frame. The elastic force $\mathbf{R}_{e,i}$ and moment $\mathbf{M}_{e,i}$ applied on node i, projected in the corotational frame *, are then given by

$$\{\mathbf{R}_{e,i}\}_* = -\sum_{j}^{N} \left([\mathbf{K}_{Ti,Tj}]_* \{\mathbf{u}_j\}_* + [\mathbf{K}_{Ti,Rj}]_* \{\boldsymbol{\beta}_j\}_* \right) \tag{16}$$

$$\{\mathbf{M}_{e,i}\}_* = -\sum_{j}^{N} \left([\mathbf{K}_{Ri,Tj}]_* \{\mathbf{u}_j\}_* + [\mathbf{K}_{Ri,Rj}]_* \{\boldsymbol{\beta}_j\}_* \right) \tag{17}$$

where the elastic displacements $\mathbf{u}_j$ and rotations $\boldsymbol{\beta}_j$ are computed from the difference between the actual position of node j and its position on the undeformed body attached to the corotational frame *. For the sake of simplicity, the computation of the elastic rotations is performed from angles between axes, assuming small relative rotations.

The corresponding generalized force on configuration parameter q_l can be written

$$Q_l^{elastic} = \sum_{i=1}^{N} \left(\mathbf{R}_{e,i} \cdot \mathbf{d}_{i,l} + \mathbf{M}_{e,i} \cdot \boldsymbol{\theta}_{i,l} \right) \tag{18}$$

6

3.4 Contribution of external forces

If we denote by $\mathbf{R}_i$ and $\mathbf{M}_i$ the total force respectively torque applied on node i of the flexible body, their contribution in the generalized force related to configuration parameter q_l is given by

$$Q_l^{ext} = \sum_{i=1}^{N} (\mathbf{R}_i \cdot \mathbf{d}_{i,l} + \mathbf{M}_i \cdot \boldsymbol{\theta}_{i,l}) \tag{19}$$

3.5 Summary

To define a flexible body, the user will have to provide

- the mass and stiffness matrices (assumed projected in the corotational frame) of the flexible body/superelement;

- the homogeneous transformation matrices giving the situation of each node with respect to the corotational frame in the undeformed configuration;

- the expression of the homogeneous transformation matrices giving the situation of each of the N nodes of the flexible body, and the one of the corotational frame, in terms of the chosen configuration paremeters; velocities and accelerations directly derive from these matrices;

- the external forces acting on each node of the flexible body.

The total contribution of the flexible body in the equation of motion related to configuration parameter q_l can then be expressed by

$$\begin{aligned} Q_l^{tot} &= \sum_{i=1}^{N} \{ (\mathbf{R}_i(-m\mathbf{a}) + \mathbf{R}_i(g) + \mathbf{R}_{e,i} + \mathbf{R}_i) \cdot \mathbf{d}_{i,l} + (\mathbf{M}_i(-m\mathbf{a}) + \mathbf{M}_i(g) + \mathbf{M}_{e,i} + \mathbf{M}_i) \cdot \boldsymbol{\theta}_{i,l} \} \\ &\quad + \mathbf{M}_*(-m\mathbf{a}) \cdot \boldsymbol{\theta}_{*,l} \end{aligned} \tag{20}$$

4 Example 1: simple pendulum

The first studied system consists of a flexible simple pendulum subjected to gravity forces. This planar flexible pendulum is attached to the reference frame (x_0, y_0) through a revolute joint. It is dropped in the gravity field from an horizontal undeformed configuration. The flexible beam characteristics[7] are provided in table 1. In this example and subsequent ones, the stiffness and mass matrices correspond to standard Euler-Bernouilli beams.

Density ρ:	7.8E-3 kg/m^3	Length L:	141.42 m
Young's modulus E:	2.1 E6 N/m^2	Section A:	9.0 m^2
Poisson's ratio v:	0.3	Moments of inertia I_y and I_z:	6.75 m^4

Tab. 1: Flexible beam characteristics from [7]

The flexible beam involves 3 frames: one at each end and the corotational frame (figure 5)

- the first frame is at the basis of the beam; its motion is defined through the homogeneous transformation matrix $\mathbf{T}_{0,1}$ and depends only on $\boldsymbol{q}_0$ which is the rotation about the z axis

$$\mathbf{T}_{0,1} = \mathbf{T}_{rotz}(\boldsymbol{q}_0)$$

- the second frame of the flexible beam is located at the end of the beam and involves 6 more DOF corresponding to the 3 translational ($\boldsymbol{q}_1$, $\boldsymbol{q}_2$, $\boldsymbol{q}_3$) and the 3 rotational ($\boldsymbol{q}_4$, $\boldsymbol{q}_5$, $\boldsymbol{q}_6$) deformation displacements of the tip of the beam, with respect to the undeformed configuration

$$\mathbf{T}_{0,2} = \mathbf{T}_{0,1} * \mathbf{T}_{disp}(L + \boldsymbol{q}_1, \boldsymbol{q}_2, \boldsymbol{q}_3) * \mathbf{T}_{rotx}(\boldsymbol{q}_4) * \mathbf{T}_{roty}(\boldsymbol{q}_5) * \mathbf{T}_{rotz}(\boldsymbol{q}_6)$$
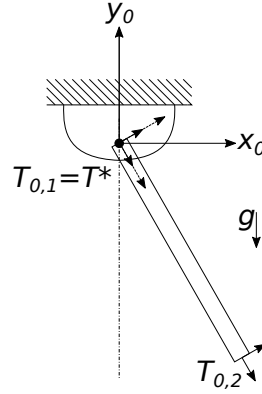
Fig. 5: Flexible simple pendulum

- the corotational frame is coincident with the first frame

$$\mathbf{T}^* = \mathbf{T}_{0,1}$$

Figure 6 shows the time history of the angular velocity ($\dot{q}_0$) at the origin and the transversal tip displacement (q_2) of the beam. A very good correspondence is observed between the vibrations retrieved from the `EasyDyn` library and those from the `AMR` software. The latter is another in-house software based on relative coordinates, the flexible bodies being implemented according to the local floating frame approach[8], with stiffening effect for beams with respect to longitudinal forces. As the rotation velocity and the deformation of the body are small, the curves perfectly match.
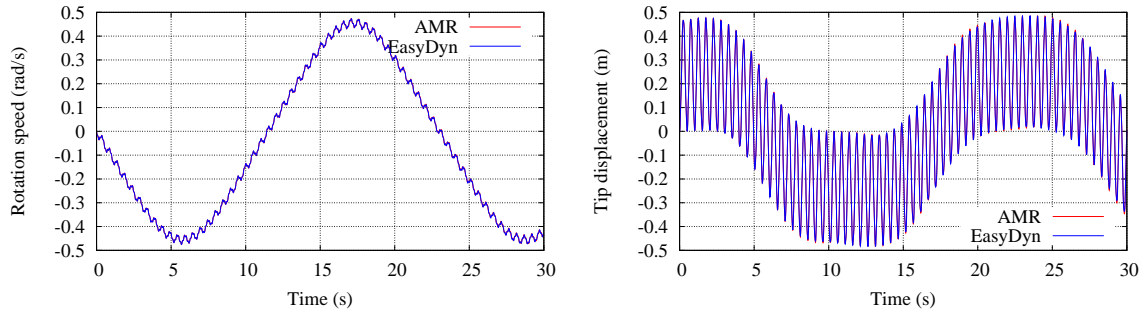
Fig. 6: Simulation results related to the flexible pendulum

5   Example 2: Hinge beam

5.1   Description of the system

The hinge beam illustrated in figure 7 was used as a benchmark in reference [7]: the flexible beam is subjected to a varying torque around the z-axis from a static initial position. The flexible beam characteristics are those already presented in table 1.

5.2   Absolute vs relative coordinates

The beam is modelled with the same frames as in the previous section. However, we also investigate the results obtained when the motion of the tip frame is defined directly with respect to the ground. In this case, the configuration parameters correspond to absolute nodal coordinates and the transformation matrix is given by

$$\mathbf{T}_{0,2} = \mathbf{T}_{disp}(\boldsymbol{q}_1, \boldsymbol{q}_2, \boldsymbol{q}_3) * \mathbf{T}_{rotx}(\boldsymbol{q}_4) * \mathbf{T}_{roty}(\boldsymbol{q}_5) * \mathbf{T}_{rotz}(\boldsymbol{q}_6)$$
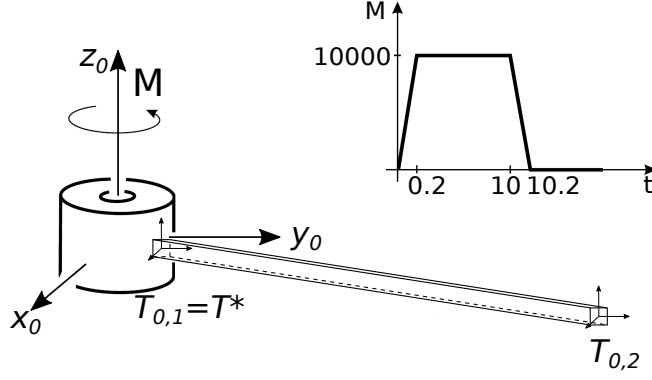
8

Fig. 7: Cardona's hinge beam: illustration and applied torque

Moreover, consistent initial conditions must be given for an initial undeformed configuration. For example

$$q_0^0=\theta \qquad q_1^0=L\cos\theta \qquad q_2^0=L\sin\theta \qquad q_6^0=\theta$$
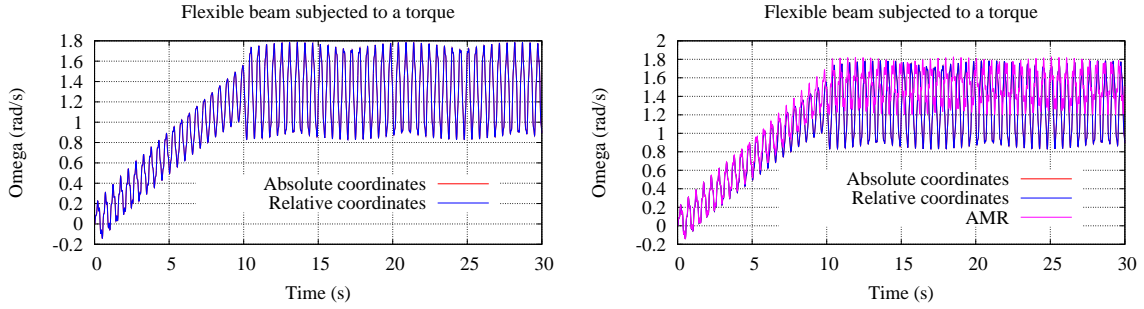
θ being equal to 0 in our case.

Fig. 8: Cardona's hinge beam: time history of basis rotation speed

Some simulation results are depicted in figure 8 in which the angular velocity at the origin of the beam is plotted. Despite a totally different conditioning for the transformation homogeneous matrix $T_{0,2}$, the two curves perfectly overlap. However, the results obtained from `EasyDyn` do not agree with the ones of `AMR`: the curves perfectly match at the beginning of the simulation and progressively depart from each other when the angular velocity increases. Let us note that the magnitude of the oscillation after 10 seconds is not a significant indicator as it just depends on the state of the system when the torque is released. The discrepancy can namely be explained by the unability of the corotational formulation to perfectly represent the inertia effects when the rotation velocity increases. However, as we will see, the model under `AMR` also needs some refinement to comply with the results of Cardona which is actually more detailed as the model of the beam also involves 4 internal component modes.

5.3   Modelling of the beam with 5 nodes

In order to improve the interpolation of the corotational formulation, the beam is now modelled by 5 equally spaced frames (nodes), as illustrated in figure 9. Only the planar motion is retained and the 4 remaining configuration parameters correspond to the hinge angle (q_0), the longitudinal and lateral displacements ($q_1=U$, $q_2=V$) and the rotation of the tip ($q_3=\Theta$) respectively. For a consistent comparison, the motion of the internal frames is interpolated according to the beam shape functions. For example, the shape functions in the XY plane, represented on figure 9 with dashed lines (u, v, θ) allow to calculate the displacements in terms of the relative longitudinal position $\xi = \frac{x}{L}$
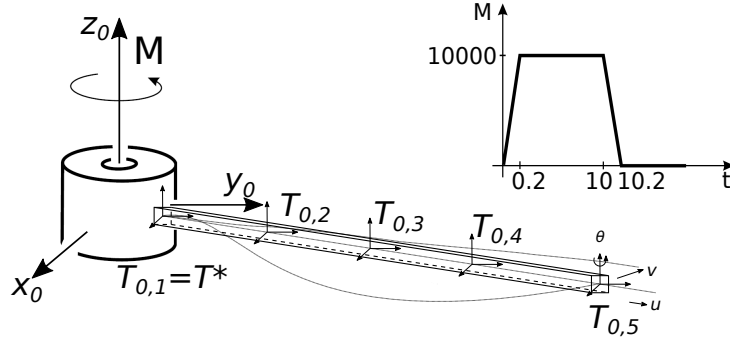
9

Fig. 9: Hinge beam with 5 nodes and 3 shape functions

1. longitudinal displacement u due to the longitudinal tip diplacement U: $u = \xi\, U$

2. lateral displacement v due to the lateral tip displacement V: $v = (3\xi^2 - 2\xi^3)V$

3. lateral displacement v due to tip rotation Θ: $v = L(\xi^3 - \xi^2)\Theta$

while local rotations can be determined from the slopes of the shape functions.

Each homogeneous transformation matrix is then written in translation and in rotation in function of the relative tip displacements, according to the shape functions and their slopes. For example, the contribution of the second frame is stated as follows:

$$\mathbf{T}_{0,2} = \mathbf{T}_{0,1} \cdot T_{disp}\left(\frac{L+q_1}{4}, \frac{5}{32}q_2 - \frac{3L}{64}q_3, 0\right) \cdot T_{rotz}\left(\frac{9}{8L}q_2 - \frac{5}{16}q_3\right) \tag{21}$$

The tracked quantity is still the angular velocity at the basis of the beam compared to the one retrieved from the `AMR` software in which one beam element composed of 2 frames is simulated (figure 10). No improvement can be observed, leading to the hypothesis that the discrepancy could be due to the geometric stiffening of the beam.
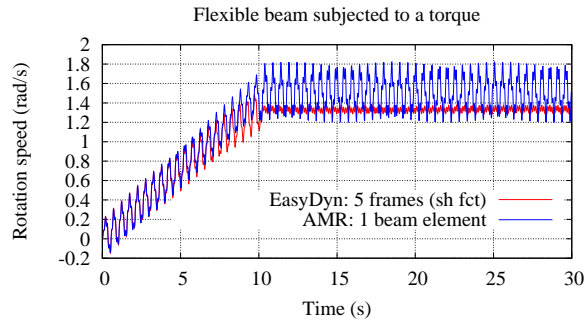

Fig. 10: Comparison `EasyDyn` vs. AMR

5.4 Modelling of the beam with 4 successive elements

In order to verify this hypothesis, the beam is modelled as the succession of 4 beam elements of a length $L/4$ (figure 11), the first nodal frame of an element corresponding to the second frame of the previous one. The corresponding kinematics allows to represent large displacements although the deformations remain small inside each element. As depicted in figure 11, the corotational frame $T*$ of each element corresponds to the first nodal frame. The model ends up with 12 transformation homogeneous matrices (but actually only 5 different ones) and 25 DOF: 6 DOF for the deformations of each beam element and 1 DOF for the hinge.
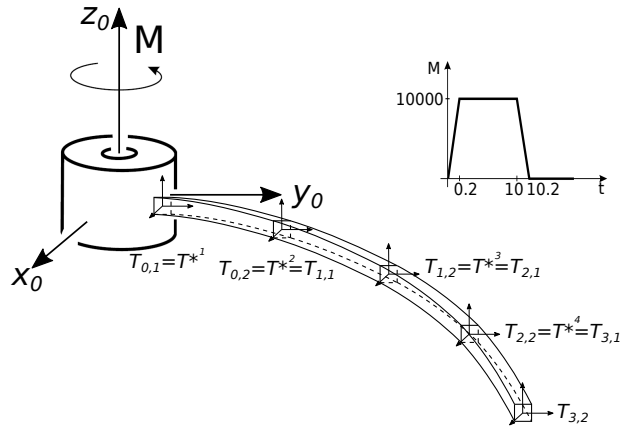
10

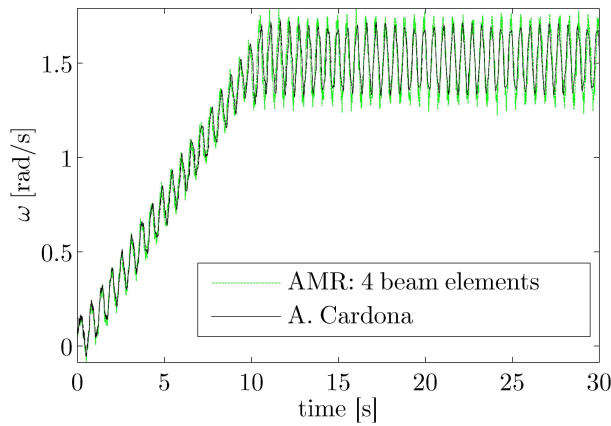Fig. 11: Hinge beam built with 4 successive elements

Fig. 12: Cardona's non-linear beam vs. AMR 4 successive elements

Figure 12 presents a comparison between the angular velocity for a hinge beam composed of 4 successive elements from `AMR` and the reference results obtained by Cardona in [9] and [7], which is a beam constituted by five equally-spaced nonlinear beam finite elements. Cardona's curve was extracted and post-treated from his original article and then superimposed to the `AMR` result. A very good agreement is now observed. Figure 13 compares the angular velocity obtained from the model with 4 successive beams by on one hand `EasyDyn` and the corotational approach and on the other hand `AMR`. The correlation is now nearly perfect although the frequency of oscillations proves to be a bit different.
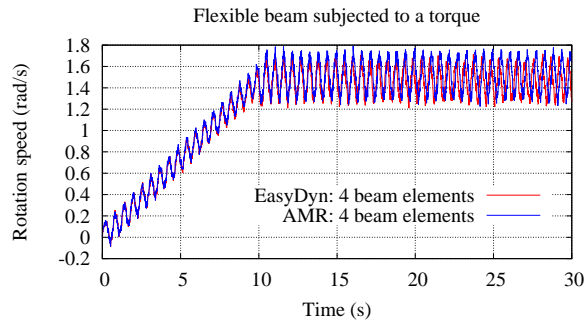

Fig. 13: `EasyDyn` 4 successive elements vs. AMR 4 successive elements

6   Example 3: slider-crank mechanism

The last considered system concerns a flexible slider-crank mechanism (figure 14) which is a closed-loop system. It is subjected to a torque M whose evolution is also displayed in figure 14. The material properties for the crank and the rod are the same as presented earlier for the hinge beam. Their lengths are respectively L_1 = 10 m and L_2 = 20 m.
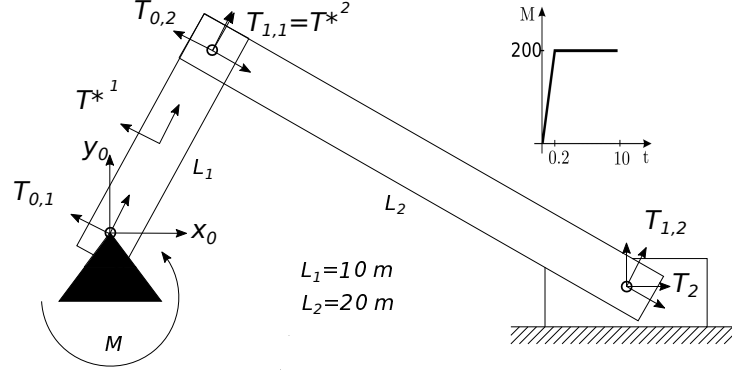

Fig. 14: Slider-crank mechanism

The slider is made of a rigid body with a mass m of 5 kg. The whole mechanism gathers a total of 7 DOF, from which the homogeneous transformation matrices are defined, giving in the same time their interpretation

$$
\begin{aligned}
\mathbf{T}_{0,1} &= \mathbf{T}_{rotz}(\boldsymbol{q}_0) \\
\mathbf{T}_{0,2} &= \mathbf{T}_{0,1} \cdot T_{disp}(L_1 + \boldsymbol{q}_1, \boldsymbol{q}_2, 0) \cdot T_{rotz}(\boldsymbol{q}_3) \\
\mathbf{T}_{1,1} &= \mathbf{T}_{0,2} \cdot T_{rotz}(\boldsymbol{q}_5) \\
\mathbf{T}_{1,2} &= \mathbf{T}_2 \cdot T_{rotz}(\boldsymbol{q}_6) \\
\mathbf{T}_2 &= \mathbf{T}_{disp}(\boldsymbol{q}_4, 0, 0)
\end{aligned}
$$

It turns out that the motion of the crank is defined in terms of the hinge angle q_0 and the tip deformations q_1, q_2 and q_3. On the contrary, frame 1.1 of the rod is defined by a relative rotation q_5 with respect to frame 0.2, while the motion of frame 2.2 is defined as a relative rotation q_6 with respect to the center of mass of the slider. The motion of the slider is defined from the only configuration parameter q_4 i.e; its X coordinate.

In the case of a closed loop system like the spring-damper, introducing flexible bodies becomes an advantage: thanks to the elastic properties of bodies which act somehow like springs, the loops do not have to be specifically solved. Due to the possibility to use relative or absolute coordinates, configuration parameters can be found, which can describe the kinematics without having to solve for intermediary parameters from loops conditions[2]. In the finite element community, the same effect can be obtained by assembly: common node displacements are merged in a single parameter.

Again, the results will be compared to AMR and, for the purpose of illustration, two different options will be tested with respect to the position of the corotational frame: at the origin of the crank (frame 0.1) or as an average position of frames 0.1 and 0.2, as

$$
\mathbf{T}^* = \mathbf{T}_{rotz}(\boldsymbol{q}_0) \cdot T_{disp}\left(\frac{L_1 + \boldsymbol{q}_1}{2}, \frac{\boldsymbol{q}_2}{2}, 0\right) \cdot T_{rotz}\left(\frac{\boldsymbol{q}_3}{2}\right)
$$

Figure 15 shows the rotation velocity of the origin of the crank ($\dot{q}_0$) for both options. Generally speaking, the results obtained with the corotational frame at the center of the crank show a better agreement with AMR. This is consistent with Cardona's paper [7] which states that *the more the corotational frame is close to the center of gravity, the less the kinetic energy is degraded and the more the results are accurate.*

It also appears that the system undergos larger vibrations with the corotational approach implemented under EasyDyn, as confirmed by figure 16 which depicts the time history of the elastic displacement and rotation of the
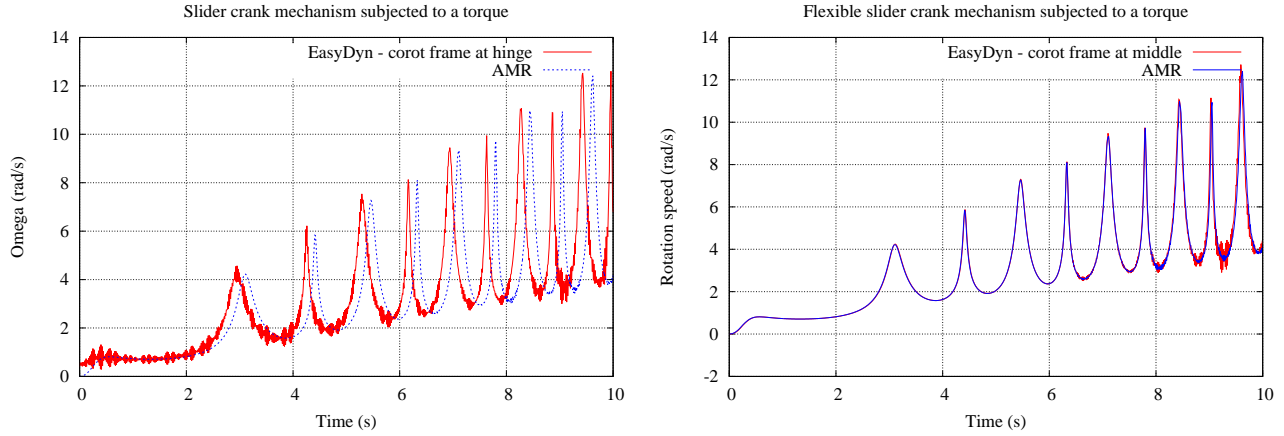
Fig. 15: Slider crank simulation with corotational frame at the origin (left) or at the middle (right) of the crank
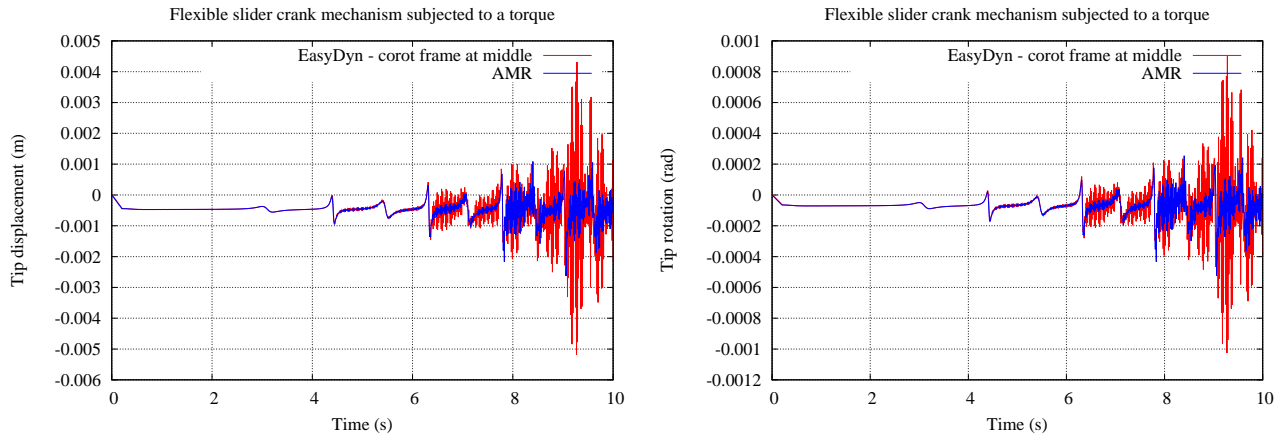

Fig. 16: Deformation of the crank: comparison between `AMR` and `EasyDyn` with the corotational frame at the middle of the crank

tip of the crank. This can be due to the integration method. Some numerical damping has to be introduced in `AMR` due to the presence of constraints.

7 Conclusions

This paper presented the extension of the framework `EasyDyn` to the simulation of flexible bodies. This work was motivated by a new project about stability of robotic machining where the contribution of the flexibility of the robot members cannot be ignored.

The kinetics of flexible bodies is introduced through the so-called co-rotational approach, which is based on an expression of the kinetic energy from the mass matrix of the finite element model of the considered body, and the nodal velocities expressed in a frame rotating with the body. Although it is not the most consistent formulation, it was found to be naturally adapted to the philosophy of minimal coordinates, minimizing the implementation effort. It is also convenient for the application, where deformations and rotation speeds are small. Only superlements are considered, the stiffness and mass matrices being potentially retrieved from any finite element software.

The paper presented the construction of the equations of motion, whose form presents several similarities with the ones related to rigid bodies. Thanks to some examples, the implementation was validated by comparison with literature and another in-house software based on relative coordinates. Some modelling issues were addressed in parallel, like the influence of the number of elements or the location of the corotational frame. As expected, the limitations of the corotational approach appear when the deformations or the rotation velocities increase.

13

Acknowledgements

References

[1] W. Schiehlen, *Multibody System Handbook*. New York, USA: Springer-Verlag, 1990.

[2] M. Hiller and A. Kecskeméthy, "Dynamics of multibody systems with minimal coodinates," in *Computer-Aided Analysis of Rigid and Flexible Mechanical Systems* (M.F.O. Seabra Pereira and J.A.C. Ambrosio, eds.), vol. 268 of *NATO ASI*, pp. 61–100, Dordrecht, the Netherlands: Kluwer Academic Publishers, 1994.

[3] O. Verlinden, L. Ben Fékih, and G. Kouroussis, "Symbolic generation of the kinematics of multibody systems in easydyn: From mupad to xcas/giac," *Theor. Appl. Mech. Lett.*, vol. 3, no. 013012, 2013.

[4] Kouroussis G., Verlinden O., Rustin C., and Bombled Q, "EasyDyn: Multibody open-source framework for advanced research purposes," in *Proceedings (on CD) of the ECCOMAS Thematic Conference Multibody Dynamics*, (Brussels, Belgium), July 2011.

[5] F. Ducobu, E. Rivière, and E. Filippi, "Dynamic simulation of the micro-milling process including minimum chip thickness and size effect," *Key Engineering Materials*, vol. 504, pp. 1269–1274, 2012.

[6] A. Cardona and M. Géradin, "Modelling of superelements in mechanism analysis," *International Journal for Numerical methods in Engineering*, vol. 32, pp. 1565–1593, 1991.

[7] A. Cardona, "Superelements modelling in flexible multibody dynamics," *Multibody System Dynamics*, vol. 4, pp. 245–266, 2000.

[8] O. Verlinden, P. Dehombreux, and C. Conti, "A new formulation for the direct dynamic simulation of flexible mechanisms based on the newton-euler inverse method," *International Journal for Numerical methods in Engineering*, vol. 37, pp. 3363–3387, 1991.

[9] Cardona A. and Géradin M., "A beam finite element nonlinear theory with finite rotations," *Internat. J. Numer. Methods Engrg*, vol. 26, pp. 2403–2438, 1988.